

Supplement of Clim. Past, 14, 2071–2087, 2018
<https://doi.org/10.5194/cp-14-2071-2018-supplement>
© Author(s) 2018. This work is distributed under
the Creative Commons Attribution 4.0 License.



Supplement of

Climate evolution across the Mid-Brunhes Transition

Aaron M. Barth et al.

Correspondence to: Aaron M. Barth (abarth@ehc.edu)

The copyright of individual parts of the supplement might differ from the CC BY 4.0 License.

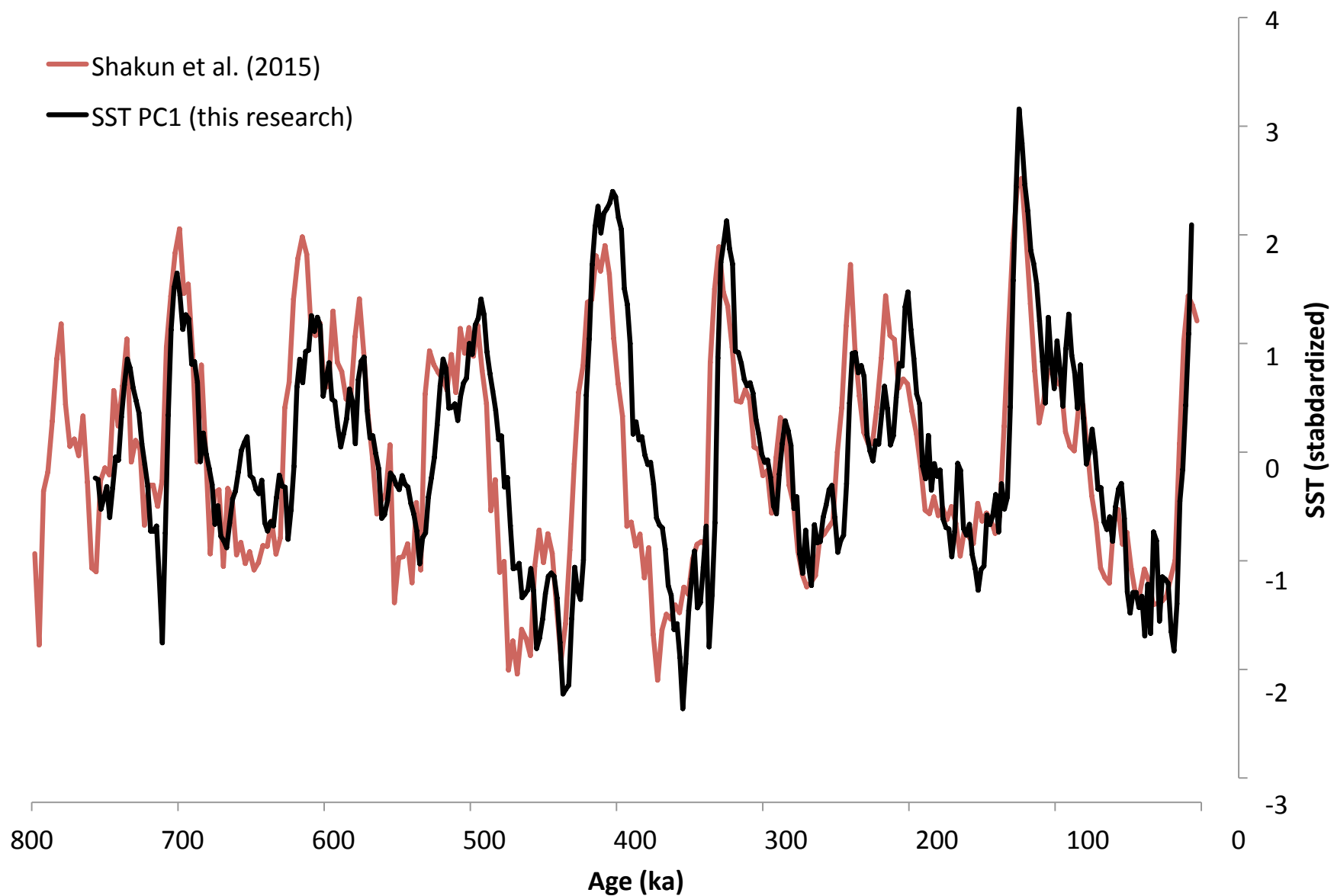


Figure S1 - Comparison of sea-surface temperature results. Results of a sea-surface temperature stack ($n = 49$; red; Shakun et al., 2015) and the first principal component of our sea-surface temperature analysis ($n = 15$; black).

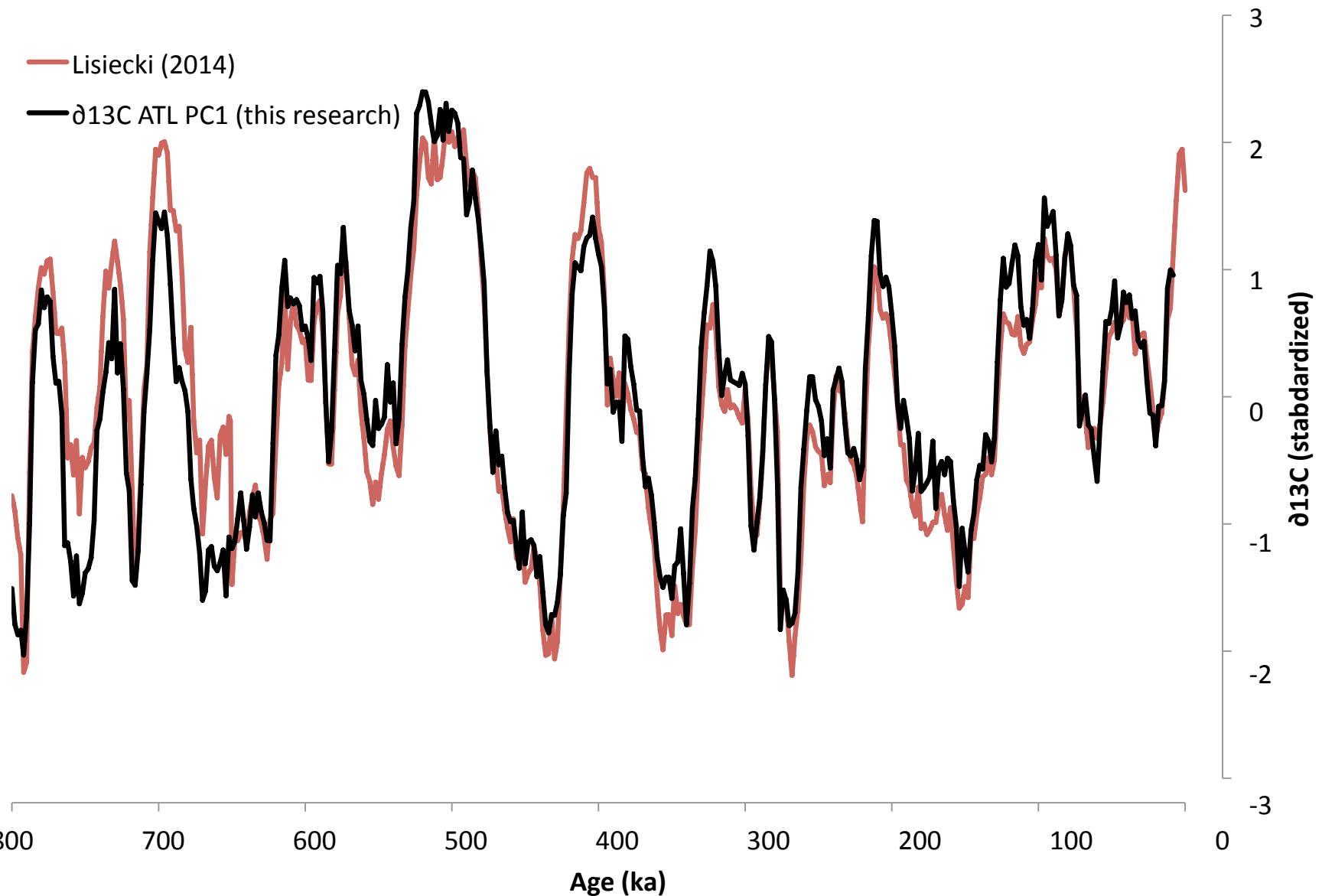


Figure S2 - comparison benthic carbon isotope results. Results of a benthic $\delta^{13}\text{C}$ stack ($n = 46$; red; Lisiecki, 2014) and the first principal component of our global benthic $\delta^{13}\text{C}$ analysis (black).

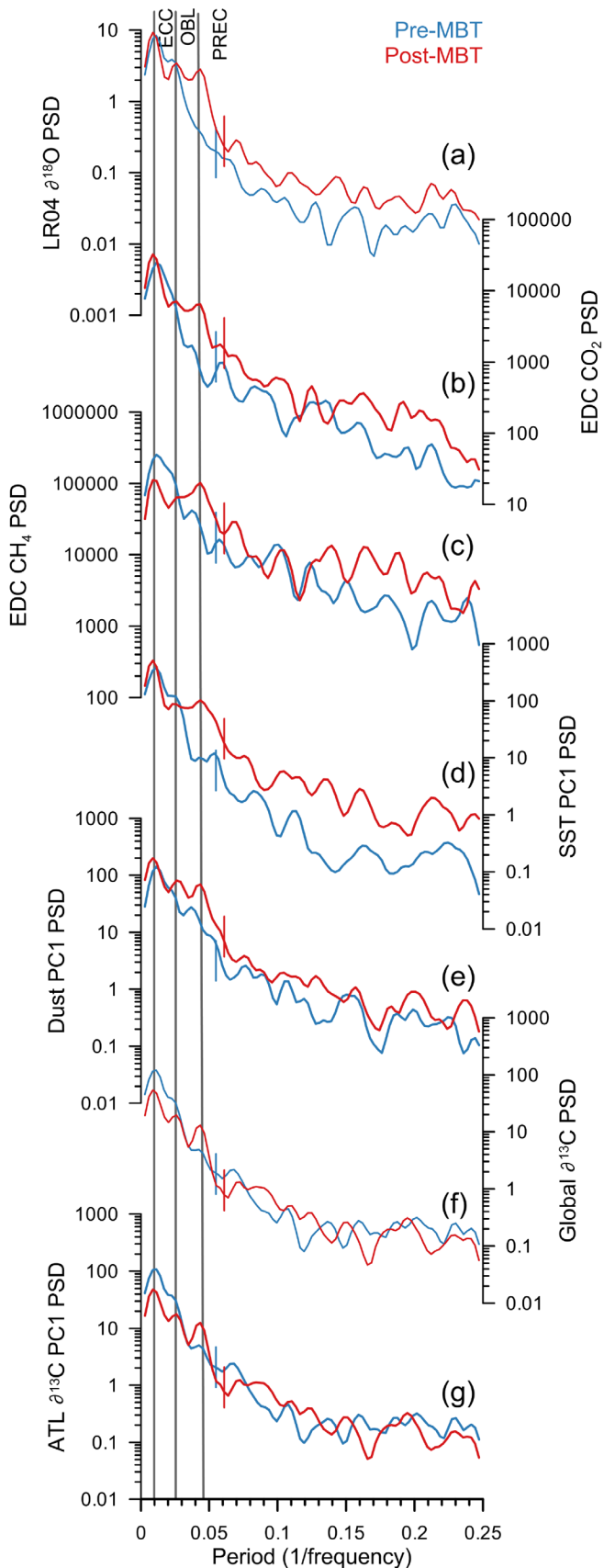


Figure 3 – Spectral power analyses. Power spectral density plots of major climate variables. Blue plot represents the pre-MBT time interval (800-450 ka). Red plot represents the post-MBT (350-8 ka). Vertical lines represent the dominant Milankovitch periods at 100-, 41-, and 23-kyr. **a**, LR04 benthic oxygen isotope stack. **b**, EPICA Dome C CO_2 . **c**, EPICA Dome C CH_4 . **d**, Sea-surface temperatures PC1. **e**, Dust PC1. **f**, Global $\delta^{13}\text{C}$ PC1. **g**, Atlantic $\delta^{13}\text{C}$ PC1.

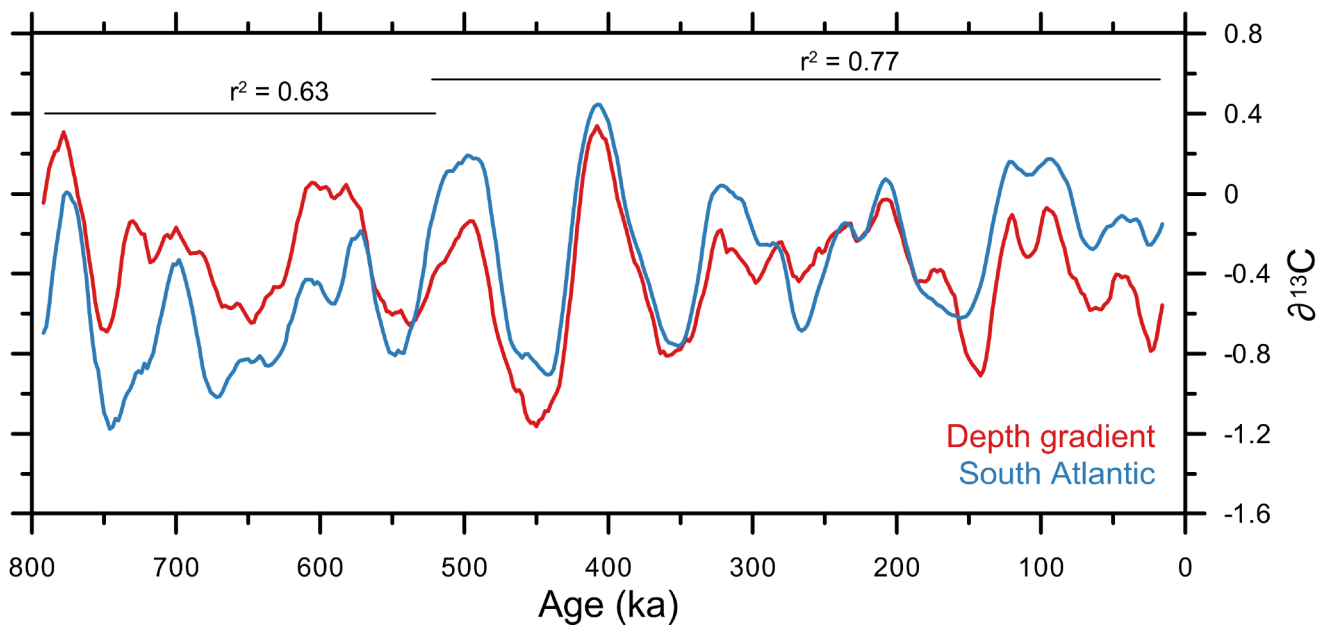


Figure 10 –North Atlantic depth gradient and South Atlantic $\delta^{13}\text{C}$. Depth gradient of the North Atlantic $\delta^{13}\text{C}$ records (Deep minus Intermediate; red) compared with the Deep South Atlantic $\delta^{13}\text{C}$ stack (blue). Each record has been smoothed using a 9-point moving average. Both are plotted in $\delta^{13}\text{C}$ space to highlight the similarity in values once the isotopic influence of the Intermediate North Atlantic is removed. Horizontal lines indicate a period of lower correlation ($r^2 = 0.63$) prior to MIS 15, and higher correlation ($r^2 = 0.77$) after the MIS 15.

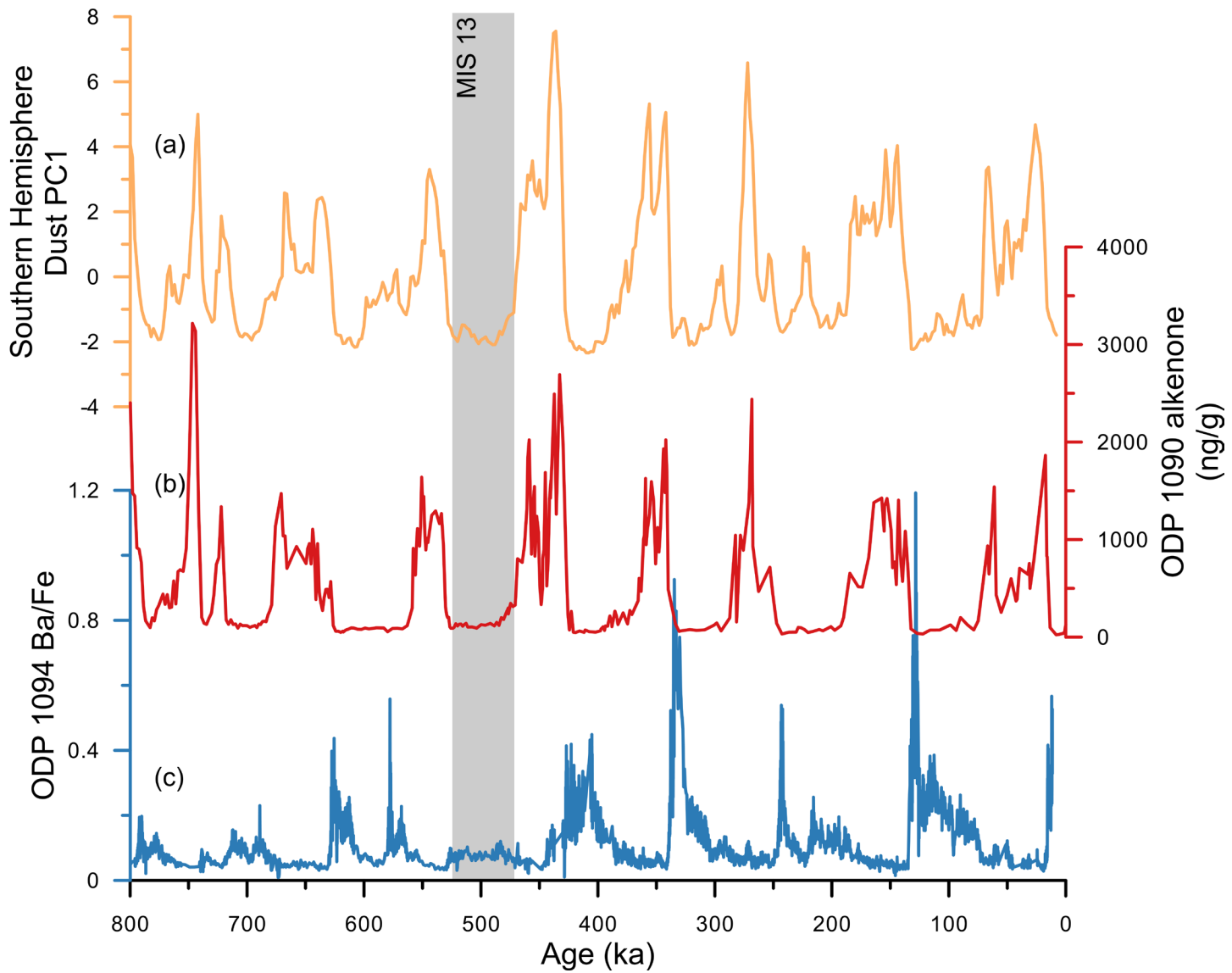


Figure 13 – Dust and productivity. **a**, the first principal component of southern dust (orange). The y-axis has been inverted to show interglacial periods as up. **b**, Alkenone record of export productivity from the Subantarctic Zone (ODP 1090; Martinez-Garcia et. al, 2009; red). **c**, Ba/Fe ratios show export productivity from the Antarctic Zone (ODP 1094; Jaccard et al., 2013; blue). The vertical gray box highlights a period of little to no export productivity or dust during MIS 13.

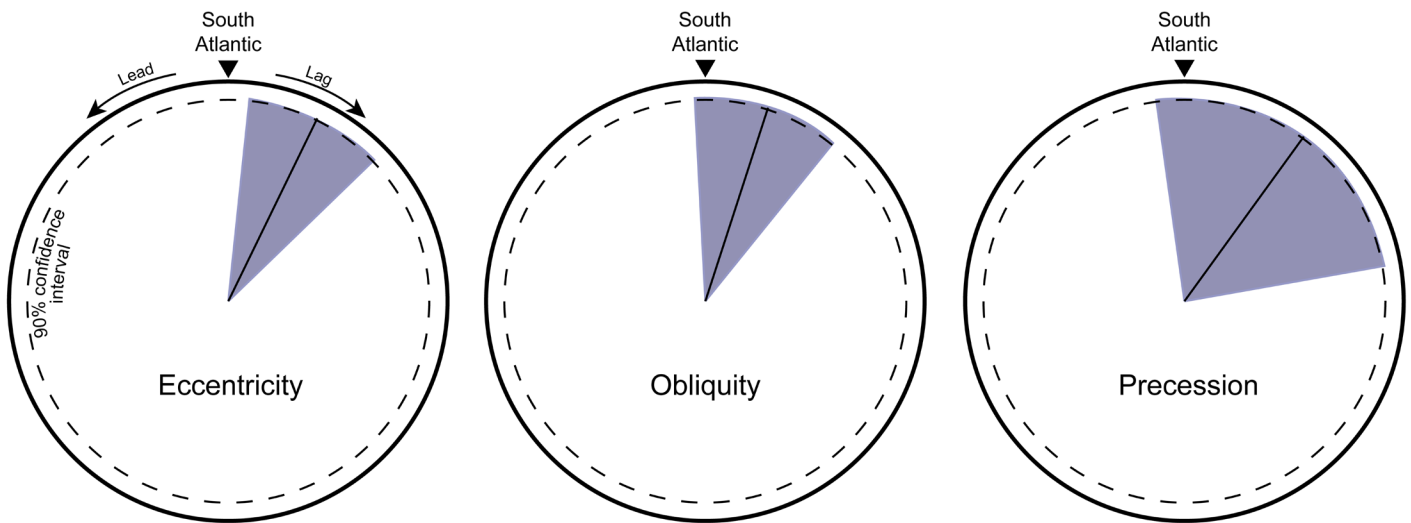


Figure 16 – Post-MBT $\delta^{13}\text{C}$ phase wheels. Phase wheels for each of the Milankovitch cycles (eccentricity, obliquity, and precession) between the North and South Atlantic $\delta^{13}\text{C}$ regional stacks. The arrow at the top of each wheel shows an in-phase relationship of the North Atlantic with the South Atlantic in that frequency band. Values to the right indicate a lag by the North Atlantic relative to the South Atlantic. Values to the left indicate a lead by the North Atlantic relative to the South Atlantic. Purple shading indicates the uncertainty in each relationship. Dotted line highlights the 90% confidence interval for each frequency.

Table S1 - Variance tests

Data Set	Variable	Period	Variance ^a	F-test ^b
SST_PC1	SST	Post-MBT	8.9681	Reject
SST_PC1	SST	Pre-MBT	6.5399	
SST_PC2	SST	Post-MBT	1.8564	
SST_PC2	SST	Pre-MBT	1.2808	
EDC CO ₂	CO ₂	Post-MBT	619.6373	Reject
EDC CO ₂	CO ₂	Pre-MBT	467.1198	
$\delta^{13}\text{C}$ Atlantic PC1	$\delta^{13}\text{C}$	Post-MBT	0.9950	Reject
$\delta^{13}\text{C}$ Atlantic PC1	$\delta^{13}\text{C}$	Pre-MBT	1.9414	
$\delta^{13}\text{C}$ Atlantic PC1 no MIS 13	$\delta^{13}\text{C}$	Post-MBT	0.9950	Reject
$\delta^{13}\text{C}$ Atlantic PC1 no MIS 13	$\delta^{13}\text{C}$	Pre-MBT	1.9414	
$\delta^{13}\text{C}$ Atlantic PC2	$\delta^{13}\text{C}$	Post-MBT	0.2365	Reject
$\delta^{13}\text{C}$ Atlantic PC2	$\delta^{13}\text{C}$	Pre-MBT	0.3378	
$\delta^{13}\text{C}$ Pacific PC1	$\delta^{13}\text{C}$	Post-MBT	0.2283	Reject
$\delta^{13}\text{C}$ Pacific PC1	$\delta^{13}\text{C}$	Pre-MBT	0.4317	
$\delta^{13}\text{C}$ Global	$\delta^{13}\text{C}$	Post-MBT	1.1744	Reject
$\delta^{13}\text{C}$ Global	$\delta^{13}\text{C}$	Pre-MBT	2.1739	
$\delta^{13}\text{C}$ Global	$\delta^{13}\text{C}$	Post-MBT	1.1744	Reject
$\delta^{13}\text{C}$ Global	$\delta^{13}\text{C}$	Pre-MBT	2.1739	
LR04 $\delta^{18}\text{O}$	$\delta^{18}\text{O}$	Post-MBT	0.1965	Reject
LR04 $\delta^{18}\text{O}$	$\delta^{18}\text{O}$	Pre-MBT	0.1572	
Dust Global	Dust	Post-MBT	4.5498	Reject
Dust Global	Dust	Pre-MBT	2.6819	
EDC CH ₄	CH ₄	Post-MBT	5432.4	
EDC CH ₄	CH ₄	Pre-MBT	6012.4	
EDC Temperature	Deuterium	Post-MBT	270.1	Reject
EDC Temperature	Deuterium	Pre-MBT	116.3	
Bottom water temp.	Mg/Ca	Post-MBT	0.0105	Reject
Bottom water temp.	Mg/Ca	Pre-MBT	0.0069	

^aVariance values for the intervals "Pre-MBT" (450-800 ka) and "Post-MBT" (0-350 ka)

^bF-tests of the null hypothesis that variance in the Pre- and Post-MBT time intervals are the same

Table S2 - EOF Results

Core	EOF-1	EOF-2
<i>Sea-surface temperature</i>		
DSDP 607	2.4611	-1.4678
ODP 846	0.6214	0.1373
ODP 982	0.9055	0.1431
ODP 1143	0.5791	0.0256
ODP 1082	1.2605	-0.0162
ODP 1313	1.5653	-0.0557
ODP 722	0.6955	-0.0637
ODP 1146	0.6955	-0.0637
ODP 846	0.6214	0.1373
MD97-2140	0.3085	0.0024
MD06-3018	0.3711	0.1174
ODP 806	0.6318	0.0738
DSDP 594	1.6780	2.1688
V22-174	0.4994	-0.0700
RC13-110	0.6403	-0.2426
<i>Dust</i>		
ODP 659	0.356	0.646
ODP 1090	0.9004	-0.2768
ODP 1090	0.8957	-0.2884
CLP	-0.5902	-0.4107
PS75-074	0.8153	-0.107
PS75-076	0.8914	-0.0061
ODP 663	0.4237	0.6842
EPICA Dome C	0.8729	-0.1856
<i>Global $\delta^{13}\text{C}$</i>		
ODP 982	0.0473	-0.1403
ODP 983	0.1598	-0.1581
ODP 984	0.1412	-0.4831
DSDP 607	0.4186	0.0256
U 1308	0.3688	0.0163
DSDP 502	0.0674	-0.098
ODP 980/981	0.2748	-0.1104
ODP 664	0.3818	0.0776
ODP 925	0.3548	0.027
ODP 926	0.3949	0.0174
ODP 927	0.3886	0.0161
ODP 929	0.4186	0.0256
ODP 928	0.4069	0.0414
ODP 1090	0.3774	0.1325
ODP 1143	0.1641	-0.0143
ODP 677	0.185	-0.0199
ODP 846	0.1795	-0.0169
ODP 849	0.1901	-0.003
<i>Atlantic $\delta^{13}\text{C}$</i>		
ODP 982	0.0459	0.1404
ODP 983	0.1567	0.1579
ODP 984	0.1373	0.4838
DSDP 607	0.423	-0.0194
U 1308	0.3683	-0.0141
ODP 980/981	0.2733	0.112
DSDP 502	0.0674	0.0989
ODP 664	0.3805	-0.0756
ODP 925	0.3555	-0.0242
ODP 926	0.3964	-0.0136
ODP 927	0.39	-0.0129
ODP 929	0.423	-0.0194
ODP 928	0.408	-0.0379
ODP 1090	0.3728	-0.134
<i>Pacific $\delta^{13}\text{C}$</i>		
ODP 1143	0.5066	-0.1312
ODP 677	0.113	0.0389
ODP 846	0.1482	0.1219
ODP 849	0.2123	0.2073